Available online at www.sciencedirect.com
ScienceDirect
Scripta Materialia 57 (2007) 917–920
Scripta MATERIALIA
www.elsevier.com/locate/scriptamat

Formation of (B2 + $D0_3$) phases at $a/2\langle 100\rangle$ anti-phase boundary in an Fe–23 at.%Al–8.5 at.%Ti alloy

Chun-Wei Su, Chuen-Guang Chao and Tzeng-Feng Liu*

National Chiao Tung University, Department of Materials Science and Engineering, 1001 Ta Hsueh Road, Hsinchu 30049, Taiwan

Received 28 June 2007; revised 19 July 2007; accepted 22 July 2007
Available online 20 August 2007

The as-quenched microstructure of the Fe–23 at.%Al–8.5 at.%Ti alloy was a mixture of (A2 + $D0_3$) phases. Transmission electron microscopy (TEM) examinations indicated that when the alloy was aged at 900 °C, the size of the $D0_3$ domains increased with increasing aging time, and an A2 → (A2 + $D0_3$) → (B2 + $D0_3$) transition occurred at $a/2\langle 100\rangle$anti-phase boundaries (APBs). This feature has never been reported by other workers in the Fe–Al–Ti alloy systems.

Keywords: Iron alloys; Phase transformations; TEM; Anti-phase boundary

In order to improve the high-temperature oxidation and mechanical properties, several authors have added Ti to Fe–Al binary alloys [1–5]. Based on their results, it can be generally concluded that the addition of Ti can effectively improve these properties. In addition, the effects of Ti addition on the microstructures of Fe–Al binary alloys have also been studied by many workers [3–13]. It was reported that the addition of Ti would strongly increase the $D0_3$ → B2 and B2 → A2 transition temperatures [6–13] and expand the (A2 + $D0_3$) phase field [10–12]. Furthermore, a (B2 + $D0_3$) two-phase field was claimed to be existent in the Fe–Al–Ti ternary alloys [11–13]. It should be mentioned that the (B2 + $D0_3$) two-phase field has not been found by previous workers in the Fe–Al binary alloys [14–16]. However, the existence of a (B2 + $D0_3$) two-phase field in Fe–Al–Ti ternary alloys was confirmed principally by using X-ray diffraction and electron-probe microanalysis [11–13]. In order to clarify the microstructural revolution for the formation of the (B2 + $D0_3$) phases, a transmission electron microscopy (TEM) study was performed to investigate the phase transition in the Fe–23 at.%Al–8.5 at.%Ti alloy.

The Fe–23 at.%Al–8.5 at.%Ti alloy was prepared in a vacuum induction furnace by using pure Fe (99.9%), Al (99.9%) and Ti (99.9%). After being homogenized at 1250 °C for 48 h, the ingot was sectioned into 2 mm-thick slices. These slices were subsequently solution heat-treated at 1100 °C for 1 h and then quenched rapidly in room-temperature water. The aging process was performed at 900 °C for various times in a vacuum heat-treated furnace followed by rapid quenching. TEM specimens were prepared by a double-jet electropolisher with an electrolyte of 67% methanol and 33% nitric acid. TEM observation was performed using a JEOL JEM-2000FX transmission electron microscope operating at 200 kV. Elemental concentrations were examined by using a Link ISIS 300 energy-dispersive X-ray spectrometer (EDS). Quantitative analyses of elemental concentrations for Fe, Al and Ti were made using the Cliff–Lorimer ratio thin section method.

Figure 1(a) shows a selected-area diffraction pattern of the as-quenched alloy, revealing the presence of the superlattice reflection spots of the ordered $D0_3$ phase [17]. Figures 1(b) and (c) are (1 1 1) $D0_3$ and (2 0 0) $D0_3$ (or, equivalently, (1 0 0) B2) dark-field (DF) electron micrographs of the as-quenched alloy, exhibiting the presence of fine $D0_3$ domains with $a/2\langle 100\rangle$ APBs and small B2 domains with $a/4\langle 111\rangle$ APBs, respectively [15,16]. In Figure 1(c), a high-density of disordered A2 phase showing a dark contrast could also be seen within the B2 domains. Accordingly, the as-quenched microstructure of the alloy was a mixture of (A2 + $D0_3$) phases. This is similar to what has been reported by other workers in as-quenched Fe–(18–22.5) at.%Al–5 at.%Ti alloys [10].

When the as-quenched alloy was aged at 900 °C for a short time, the $D0_3$ domains grew with preferred

* Corresponding author. Tel.: +886 3 5712121x55316; fax: +886 3 5713987; e-mail: tfliu@cc.nctu.edu.tw

1359-6462/$ - see front matter © 2007 Acta Materialia Inc. Published by Elsevier Ltd. All rights reserved.
doi:10.1016/j.scriptamat.2007.07.023

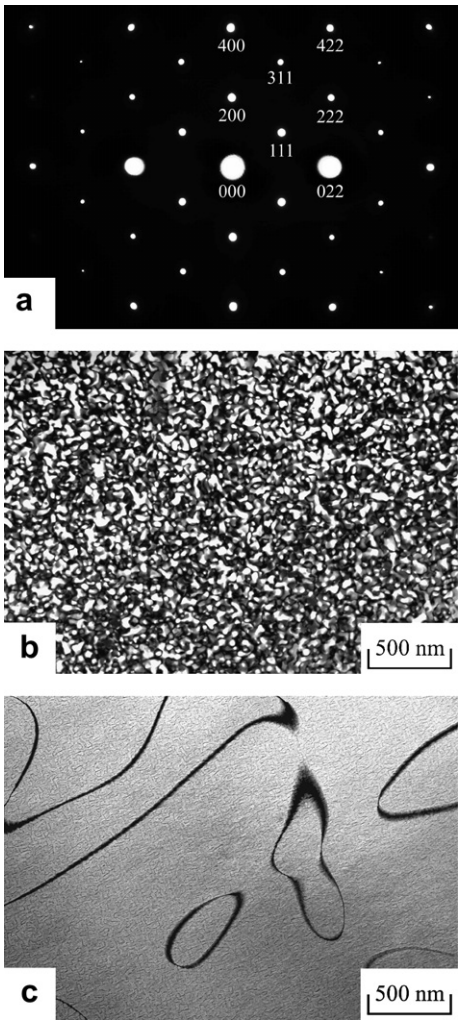

Figure 1. Electron micrographs of the as-quenched alloy: (a) a selected-area diffraction pattern. The foil normal is $[0\,1\,\bar{1}]$ ($hkl = D0_3$ phase); (b) and (c) (1 1 1) and (2 0 0) $D0_3$ DF, respectively.

orientation, as shown in Figure 2. This feature is similar to that reported by other workers in aged Fe–Al–Ti alloys [10]. In Figure 2, it is also seen that the $a/2\langle 1\,0\,0\rangle$ APBs were coated with a continuous layer of the disordered A2 phase. However, after prolonged aging at 900 °C, some fine particles started to appear within the A2 phase. Figures 3(a) and (b) are (1 1 1) and (2 0 0) $D0_3$ DF electron micrographs of the alloy aged at 900 °C for 1 h, clearly revealing that the (1 1 1) $D0_3$ DF image and (2 0 0) $D0_3$ DF image are morphologically identical. Since the (2 0 0) reflection spot comes from both the B2 and $D0_3$ phases [10,12], while the (1 1 1) reflection spot comes only from $D0_3$ phase, the fine bright particles at $a/2\langle 1\,0\,0\rangle$ APBs presented in Figures 3(a) and (b) are considered to be $D0_3$ phase. TEM examinations indicated that no evidence of the $a/4\langle 1\,1\,1\rangle$ APBs could be observed. This result seems to imply that the B2 domains would grow up to the whole grains during aging. With increasing the aging time at 900 °C, the amount of the $D0_3$ particles at $a/2\langle 1\,0\,0\rangle$ APBs increased and the disordered A2 phase decreased, as illustrated in Figure 4. Figure 5(a), a (1 1 1) $D0_3$ DF electron micrograph of the alloy aged at 900 °C for 24 h, indicates that at $a/2\langle 1\,0\,0\rangle$ APBs the amount of the $D0_3$ particles increased considerably and a dark contrast could also be detected between the particles. However, a (2 0 0) $D0_3$DF electron micrograph (Fig. 5(b)) reveals that the whole regions of the $a/2\langle 1\,0\,0\rangle$ APBs were full bright in contrast. This indicates that the dark regions at $a/2\langle 1\,0\,0\rangle$ APBs presented in Figure 5(a) should be of the B2 phase. Consequently, when the alloy was aged at 900 °C for a longer time, the microstructure at the $a/2\langle 1\,0\,0\rangle$ APBs was a mixture of $(B2 + D0_3)$ phases.

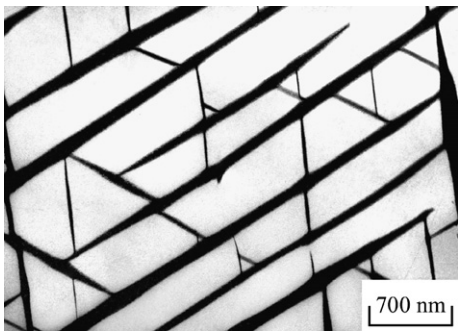

Figure 2. (2 0 0) $D0_3$ DF electron micrograph of the alloy aged at 900 °C for 0.5 h.

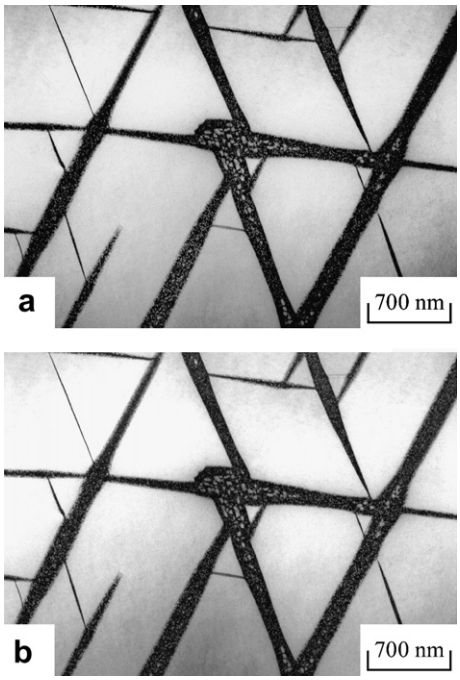

Figure 3. Electron micrographs of the alloy aged at 900 °C for 1 h. (a) (1 1 1) and (b) (2 0 0) $D0_3$ DF, respectively.

The facts that with increased aging time at 900 °C the size of the $D0_3$ domains existing in the as-quenched alloy increased and an $A2 \rightarrow (A2 + D0_3) \rightarrow (B2 + D0_3)$ transition occurred at $a/2\langle 1\,0\,0\rangle$ APBs are remarkable features in the present study. This feature has never been reported in an Fe–Al–Ti alloy system before. In order to clarify this feature, quantitative EDS analyses were undertaken. The results are shown in Table 1. It is seen in the table that when the alloy was aged at 900 °C for 0.5 h, the Al and Ti concentrations in the $D0_3$ domains

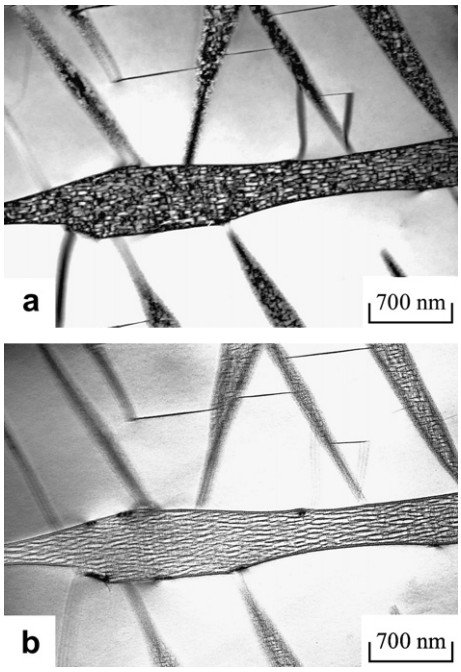

Figure 4. Electron micrographs of the alloy aged at 900 °C for 6 h. (a) (1 1 1) and (b) (2 0 0) $D0_3$ DF, respectively.

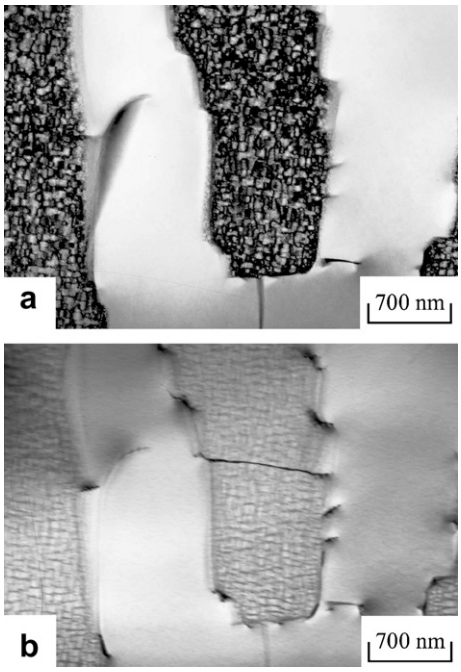

Figure 5. Electron micrographs of the alloy aged at 900 °C for 24 h. (a) (1 1 1) and (b) (2 0 0) $D0_3$ DF, respectively.

Table 1. Chemical compositions of the phases revealed by EDS

Heat treatment	Phase	Chemical composition (at.%)		
		Fe	Al	Ti
As-quenched	$A2 + D0_3$	68.3	23.1	8.6
900 °C, 0.5 h	$D0_3$ domain	62.5	25.1	12.4
	APB(A2)	75.9	19.8	4.3
900 °C, 1 h	$D0_3$ domain	63.5	24.9	11.6
	APB($A2 + D0_3$)	73.6	20.2	6.2
900 °C, 6 h	$D0_3$ domain	64.4	24.3	11.3
	APB($A2 + B2 + D0_3$)	71.6	21.5	6.9
900 °C, 24 h	$D0_3$ domain	65.1	23.8	11.1
	APB($B2 + D0_3$)	70.2	22.4	7.4

were much greater than those in the as-quenched alloy, and these concentrations were noticeably lower at $a/2\langle 1\,0\,0\rangle$ APBs. The insufficient concentrations of both Al and Ti would cause the disordered A2 phase to form at $a/2\langle 1\,0\,0\rangle$ APBs. However, along with the growth of the $D0_3$ domains, partial Al and Ti atoms would proceed to diffuse toward the $a/2\langle 1\,0\,0\rangle$ APBs. EDS analyses indicated that during the early stage of isothermal aging at 900 °C, the increased amount of Ti at $a/2\langle 1\,0\,0\rangle$ APBs was more than that of Al. This implies that, during aging, Ti redistributed first and then Al started to move appreciably. This result is consistent with that found by other workers in Fe–Al–Ti ternary alloys [18], in which they reported that the diffusion of Ti is faster than that of Al. Furthermore, it is well known that a small Ti addition in the Fe–Al binary alloys would strongly enhance the formation of the $D0_3$ phase [10–12]. Therefore, it is plausible to suggest that the drastic increase in the Ti concentration should be favorable for the formation of the fine $D0_3$ particles at $a/2\langle 1\,0\,0\rangle$ APBs, which is consistent with the observation in Figure 3. With increased aging time at 900 °C, both Al and Ti concentrations at $a/2\langle 1\,0\,0\rangle$ APBs continued to increase significantly. It is thus expected that, owing to these increases, the amount of fine $D0_3$ particles at $a/2\langle 1\,0\,0\rangle$ APBs would increase and the microstructure of the remaining regions would transform from the disordered A2 phase to B2 phase, as observed in Figures 4 and 5.

Finally, it is interesting to note that, compared with the previously established isothermal sections of Fe–Al–Ti ternary alloys at 900 °C, the chemical compositions of Fe–23.8 at.%Al–11.1 at.%Ti and Fe–22.4 at.%Al–7.4 at.%Ti obtained from the $D0_3$ domain and ($B2 + D0_3$) region in the present alloy aged at 900 °C for 24 h are just located in the $D0_3$ and the ($B2 + D0_3$) regions, respectively [12].

The as-quenched microstructure of the Fe–23 at.%Al–8.5 at.%Ti alloy was a mixture of ($A2 + D0_3$) phases. When the alloy was aged at 900 °C, the $D0_3$ domains existing in the as-quenched alloy grew and an $A2 \rightarrow (A2 + D0_3) \rightarrow (B2 + D0_3)$ transition occurred at $a/2\langle 1\,0\,0\rangle$ APBs of the $D0_3$ domains. The microstructural revolution has not previously been reported by other workers in Fe–Al–Ti alloy systems.

The authors are pleased to acknowledge the financial support of this research by the National Science Council, Republic of China under Grant NSC95-2221-E-009-086-MY3.

[1] F. Dobeš, P. Kratochvíl, K. Milička, Intermetallics 14 (2006) 1199.
[2] S.M. Zhu, K. Sakamoto, M. Tamura, K. Iwasaki, Scripta Mater. 42 (2000) 905.
[3] U. Prakash, G. Sauthoff, Intermetallics 9 (2001) 107.
[4] M. Palm, G. Sauthoff, Intermetallics 12 (2004) 1345.
[5] M. Palm, J. Lacaze, Intermetallics 14 (2006) 1291.
[6] F. Stein, A. Schneider, G. Frommeyer, Intermetallics 11 (2003) 71.
[7] L. Anthony, B. Fultz, Acta Metall. Mater. 43 (1995) 3885.
[8] M. Palm, Intermetallics 13 (2005) 1286.
[9] Y. Nishino, S. Asano, T. Ogawa, Mater. Sci. Eng. A 234–236 (1997) 271.
[10] M.G. Mediratta, S.K. Ehlers, H.A. Lipsitt, Metall. Trans. A 18 (1987) 509.
[11] G. Ghosh, in: G. Effenberg (Ed.), Ternary Alloy Systems, Springer, Berlin, 2005, pp. 426–452.
[12] I. Ohnuma, C.G. Schön, R. Kainuma, G. Inden, K. Ishida, Acta Mater. 46 (1998) 2083.
[13] S.M. Zhu, K. Sakamoto, M. Tamura, K. Iwasaki, Mater. Trans. JIM 42 (2001) 484.
[14] O. Ikeda, I. Ohnuma, R. Kainuma, K. Ishida, Intermetallics 9 (2001) 755.
[15] S.M. Allen, J.W. Cahn, Acta Metall. 24 (1976) 425.
[16] P.R. Swann, W.R. Duff, R.M. Fisher, Metall. Trans. 3 (1972) 409.
[17] C.H. Chen, T.F. Liu, Metall. Trans. A 34 (2003) 503.
[18] J. Ni, T. Ashino, S. Iwata, Acta Mater. 48 (2000) 3193.